Direct Detection of Low Molecular Weight Compounds in 2D and 3D Aptasensors by Biolayer Interferometry

Anthony Vignon, Arthur Flaget, Maxime Michelas, Mehdi Deghdir, Éric Defrancq, Liliane Coche-Guérente, Nicolas Spinelli, Angéline van der Heyden, Jérôme Dejeu

Direct Detection of Low Molecular Weight Compounds in 2D and 3D Aptasensors by Biolayer Interferometry

Anthony Vignon‡, Arthur Flaget‡, Maxime Michelas, Mehdi Djeghdir, Eric Defrancq, Liliane Coche-Guerente, Nicolas Spinelli,* Angéline Van der Heyden,* Jérôme Dejeu*

Univ. Grenoble Alpes, CNRS, DCM UMR-5250, F-38000 Grenoble, France

Supporting Information Placeholder

ABSTRACT: The direct Bio-Layer Interferometry (BLI) measurement of low molecular weight analytes (less than 200 Da) still represents a challenge particularly when low receptor densities are used. Bio-Layer Interferometry (BLI) is a powerful optical technique for label-free, real-time characterization and quantification of biomolecular interactions at interfaces. We demonstrate herein that the quantification of biomolecular recognition is possible by BLI using either 2D-like or 3D platforms for an aptamer ligand immobilization. The influence of the aptamer density on the interaction was evaluated and compared for the two sensors architectures. Despite the low molecular weight (LMW) of the analyte, BLI monitoring led to signals that are exploitable for affinity and kinetic studies even at low aptamer density. We demonstrate that the immobilization format as well as the aptamer density has a crucial influence on the determination of the recognition parameters.

Keywords: aptasensor, L-Tyrosinamide, Low Molecular Weight, small analyte, Bio-Layer Interferometry, label free detection, optical technique

Bio-layer Interferometry (BLI) has recently emerged as a powerful optical technique for the characterization and quantification of interactions between biomolecules thanks to its ease of use, particularly because it does not need any microfluidic set-up.[1] Indeed, as surface plasmon resonance (SPR), it enables real-time, label-free characterization of biomolecular interactions with the determination of affinity, kinetics and concentration using an easy-to-handle microplate format. This method, providing similar information to SPR, is based on the optical interference pattern modification induced by the optical thickness variation of the sensing layer, originating from analyte interaction with the ligand.[2] Popular applications include protein-protein and protein-molecule binding kinetics,[3] expression screening,[2] on- and off-rate screening,[1] epitope binning.[1] However, as for other optical biosensor-based techniques, the direct monitoring of low molecular weight (LMW) compounds still represents a challenge[4] and is not widespread. Indeed, the difference in the measured parameters (mass, thickness …) induced by LMW compound recognition is often modest. High surface density of ligand is an alternative to increase the detected signal, and consequently, 3D platforms (using brush-like polymer matrixes for example) are preferred to 2D sensors for ligand immobilization.[5-7] In this context, the lowest molecular weight compounds detected by BLI were the metformin (129 Da)[5] and the 3,4-dihydroxyl-phenyl lactic acid (198 Da),[7] using a 3D matrix (or SSA sensors). The lightest compound detected using a monolayer (2D or SA sensors) is CK-636 (284 Da)[8] and this architecture is generally limited to higher molecular weight compounds.[9] A promising strategy for the direct detection of LMW compounds is the use of nucleic acid aptamers as biorecognition element.[10, 11] Indeed, an interesting feature of aptamers is that in some cases the binding with the target results in a structural transition which can be exploited for transduction.[12-14] Aptamers are single-stranded oligonucleotides able to bind many types of targets (including small molecules, proteins, and whole cells) with high affinity and selectivity. Selected from a combinatorial library of oligonucleotides using the systematic evolution of ligands by exponential enrichment (SELEX) process, they show remarkable recognition properties and stabilities. Therefore, aptasensors have demonstrated their useful applications for the real time monitoring of low molecular weight molecules such as pollutants,[15] recreational drugs[16] and toxins[17] in complex media. However, examples of BLI aptasensors for the direct detection of LMW analytes are seldom reported and focused on marine toxins[18-20] with molecular weights higher than 411 Da.[18]

The present works report on the direct monitoring of L-Tyrosinamide (L-Tym), 180 Da, to explore the limits of Bio-Layer interferometry (BLI). Indeed, we have recently demonstrated that the L-Tym/aptamer interaction is detectable by using QCM-D[21] or SPR,[22] and that surface density of the aptamer strongly impacted the measured K_D.[23] Interestingly, the aptamer conformational transition upon L-Tym recognition contributed to the signal intensities measured by these two techniques. We demonstrate herein the direct detection by BLI of the interaction of the L-Tym analyte even with 2D aptasensors. We also study the impact of the type of platform (i.e. 2D or 3D) and grafting density on the recognition parameters.

The evaluation of the interaction between L-Tym and the aptamer (Apt_{49}) was performed on aptasensors based either on a 2D-like or a 3D platform. The biotinylated aptamer was immobilized on commercially available streptavidin-coated sensors SA for the 2D-like platform and SSA for the 3D platform. These two types of sensors display different quantities and spatial distributions of biotin binding sites. Aptamer density on each platform was modulated via the use of various concentrations of aptamer solutions and contact durations with the sensor.

As depicted on Figure 1, the signals recorded for L-Tym concentrations ranging from 5 to 150 µM, after double referencing procedure, display curved profiles reaching steady-state within 100s for both types of sensors and for all aptamer densities tested. Signal return to the baseline level upon rinsing with buffer confirmed the reversibility of the interaction. No signal variations were observed for similar incubations with L-Tym performed on reference surfaces composed of a random DNA sequence immo-

bilized at a saturating level on both SA and SSA sensors (Figure S1A). These controls demonstrated that L-Tym binds specifically to Apt_{49} and that non-specific interactions did not interfere with the recognition process. The specificity of the interaction was also tested by incubating 1 mM of the D-Tym enantiomer with saturated aptamer and reference surfaces for which no signal was observed (Figure S2).

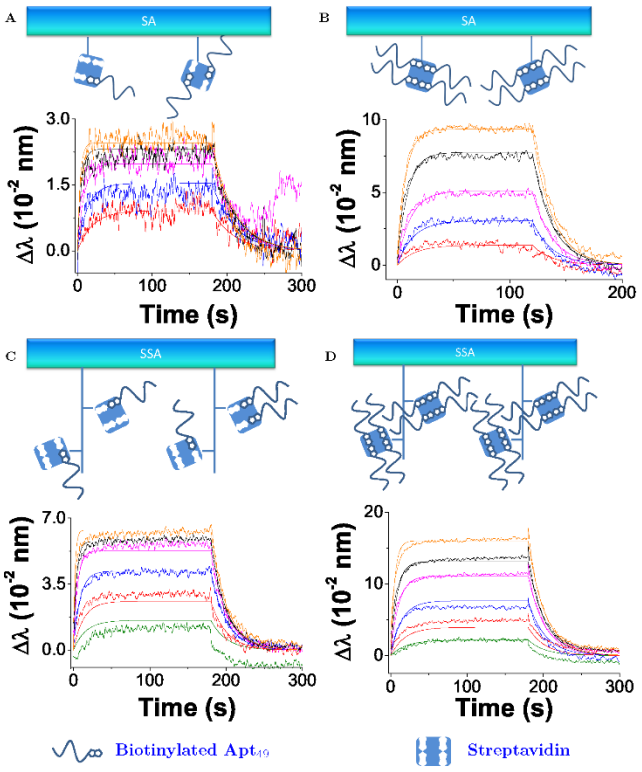

Figure 1: Schematic representation of Apt_{49} functionalized sensors and examples of sensorgrams recorded on each of them upon the addition of L-Tym at 5 (green, only for SSA), 10 (red), 25 (blue), 50 (pink), 100 (black) and 150 µM (orange). (A) low aptamer density on SA; (B) high density of aptamer on SA; (C) low density of aptamer on SSA and (D) high density of aptamer on SSA.

A good fitting of the association and dissociation phases of the sensorgrams with a 1:1 interaction model was observed which is in good agreement with the binding mechanism of this interaction (Figure 1, S3 and S4).[24] Indeed, as the recognition induces simultaneously the binding of the analyte and the aptamer folding, a two-state model (binding followed by conformational transition) is not appropriate. The fitting allows the extraction of the maximal recognition signal ($\Delta\lambda_{L,max}$) and the thermodynamic dissociation constant (K_D), calculated from the kinetic rate constants of association (k_{on}) and dissociation (k_{off}).

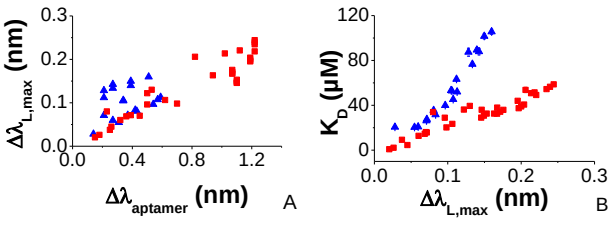

Figure 2: A) Maximal recognition signal ($\Delta\lambda_{L,max}$) versus the signal recorded at the end of the aptamer immobilization ($\Delta\lambda_{aptamer}$) and B) dissociation equilibrium constant K_D *versus* the maximal intensity of the recognition signal. Blue triangles: SA sensor and red squares: SSA sensor.

Figure 2A represents the variation of $\Delta\lambda_{L,max}$ versus the signal recorded at the end of the aptamer immobilization $\Delta\lambda_{aptamer}$. While a global increasing tendency could be observed for both sensors, the variations of $\Delta\lambda_{L,max}$ were not proportional to the $\Delta\lambda_{aptamer}$ signal. Indeed, for example on a SA sensor with $\Delta\lambda_{aptamer}$ of 0.27 nm, $\Delta\lambda_{L,max}$ ranged from 0.06 to 0.14 nm. The interferometry signal depends on the phase shift of the incident light, between the internal reference interface and the sensor extremity. This phase shift is influenced by the thickness and density of the sensing layer. A small variation of the aptamer layer thickness could induce a change in phase shift and result in a $\Delta\lambda_{aptamer}$ variation. A hypothesis to explain the difference in $\Delta\lambda_{L,max}$ for similar $\Delta\lambda_{aptamer}$ is the inhomogeneous orientation of streptavidin within the surface of the sensors. The fact that the orientation of the aptamer strands is probably random could greatly influence the thickness of the final aptasensor. However, $\Delta\lambda_{L,max}$ is correlated to the aptamer surface coverage. It could thus be considered that $\Delta\lambda_{L,max}$ reflected more adequately the density of the aptamer on the sensors surface than $\Delta\lambda_{aptamer}$. In agreement with the different density of biotin binding sites of the sensors, higher $\Delta\lambda_{L,max}$ could be obtained on SSA sensors (0.25 nm) compared to SA sensors (0.15 nm). The lowest values of $\Delta\lambda_{L,max}$ were almost equivalent for both sensors (0.028 nm for SA and 0.020 nm for SSA).

To explore the influence of the aptamer surface density on the measured affinity, the thermodynamic dissociation constant K_D is represented versus $\Delta\lambda_{L,max}$, (Figure 2B). For both sensors, K_D increased with $\Delta\lambda_{L,max}$ but two profiles can be distinguished. Indeed, K_D varied almost linearly from 1 to 60 µM for the SSA sensor when $\Delta\lambda_{L,max}$ varied from 0.020 to 0.25 nm. The affinity decreased when the aptamer density increased. Indeed, an increase of aptamer density can generate steric hindrance that could hamper the aptamer folding required for the recognition.[23]. For the SA sensors a quasi exponential variation was observed with K_D ranging from 20 to 110 µM for $\Delta\lambda_{L,max}$ values varying from 0.028 nm to 0.15 nm. Owing to the lower thickness of the SA sensing layer, a small increase of density could induce higher steric hindrance compared to SSA. Interestingly, the K_D values obtained on SA sensors are concordant with a previous SPR study performed using asimilar type of sensor (2D immobilization of aptamer),[23] giving K_D values from 110µM to 20 µM. It should be noted that similarities between affinities measured by BLI and SPR were also observed previously for molecules with a higher molecular weight.[7, 25, 26] For the highest surface coverage, the maximum measured K_D values are about two and one orders of magnitude higher, for SA and SSA sensors respectively, than those measured by homogeneous techniques such as isothermal calorimetry, fluorescence polarization or electrochemistry (1.75-3.2 µM). [24, 27, 28] This difference could be explained by the surface crowding generated by the high density of the aptamer on the sensor, which hinders the conformational transition required for the formation of the aptamer/target complex. In contrast, for lower surface coverage the K_D values are higher of only one order of magnitude for SA sensors and concordant for SSA sensors. This concordance of the K_D value for SSA sensors could be attributed to an optimal aptamer density thanks to the 3D matrix that improves the aptamer folding and offers a better accessibility of the recognition domain. This result also supports the fact that the biotin/streptavidin linkage of the aptamer with the sensor preserves the aptamer flexibility.

To develop a sensor, the affinity of the ligand for the target is as important as the sensitivity. The affinity was optimal for the lowest aptamer densities immobilized on the sensor, but the sen-

sor response to L-Tym depended on the sensor type. For SA at the lowest aptamer density, the maximal recognition signal was very weak (around 0.025 nm, Figure 1A) and sensorgrams still depended on the analyte concentration. However, no exploitable signal could be detected for concentrations lower than 10 µM, for which a signal of 0.007 nm was recorded (Figure 1A). For quantification purposes, SSA sensors were therefore more appropriate than SA sensors as they provided higher signals and exhibited lower limit of detection (LOD) and limit of quantification (LOQ) (Table S1). When the aptamer density increased, the LOQ slightly decreased from 8.2 µM to 6.0 µM. However, while higher aptamer density on the sensor increased the responses, they also hampered the affinity (Figure S5).

To have further insights on the K_D variations, the kinetic rate constants were also analyzed (Figure 3).

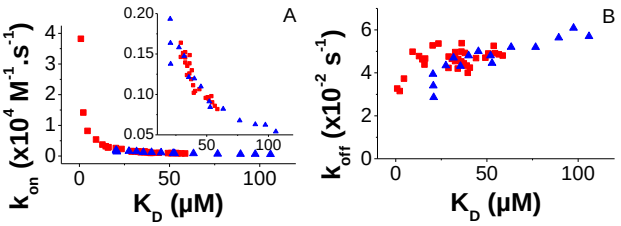

Figure 3: Variation of the kinetic rate constant: A) k_{on} and B) k_{off} for the SA (blue triangle) and the SSA (red square) sensor versus the equilibrium dissociation constant. The insert represents the enlarged part for k_{on} values below to 0.2x10^4. M^{-1}.s^{-1}.

A strong influence of aptamer density on k_{on} was observed for both sensors, Figure 3A. Indeed, k_{on} decreased upon increase of K_D (*i.e.* upon increase of the aptamer density) whereas k_{off} stayed constant at around 0.05 s^{-1}. At aptamer saturated coverage of the SA sensor, k_{on} was near 500 M^{-1}.s^{-1} and reached 2000 M^{-1}.s^{-1} for the lowest aptamer density. The latter observation is consistent with the previous hypothesis that the aptamer folding is facilitated when aptamer density decreased. Indeed, an increase of the spacing between aptamer molecules reduced steric hindrance and consequently led to a faster binding of the *L*-Tym by the aptamer. On the contrary, unfolding of the aptamer was not disturbed by the aptamer density. It is noteworthy that the kinetic rate constant variations (k_{on} and k_{off}) obtained by BLI were concordant with values previously measured by SPR on the same type of sensor, *i.e.* 2D aptamer layer (Figure S5).[22] The latter fact demonstrates that this observation (*i.e* the strong influence of k_{on} on the K_D) is undoubtedly not technique dependent.

The kinetic rate constants on SA sensors were in good agreement with those obtained on SSA sensor as shown on Figure 2 A and B. The better affinity observed on the SSA sensor at low aptamer density was also explained by an increase of the k_{on} at 40000 M^{-1}.s^{-1} for the best affinity. This value is 20 times higher than on SA sensors at the lowest aptamer density that yields detectable signals. This is consistent with the hypothesis that the folding of the aptamer was less impeded on the SSA sensor at low aptamer density. Indeed, spacing between aptamers provided by the 3D matrix reduced steric hindrance and thus allowed a faster binding of the *L*-Tym. These results suggest that the critical step for the *L*-Tym recognition by the aptamer is the association step, which could be disrupted by an important aptamer density leading the strands to hinder each other.

In conclusion, we have demonstrated, for the first time, that the direct detection of small molecules (less 200 Da) is possible by Bio-Layer Interferometry with either 2D-like or 3D platforms. The interferometry signal due to analyte recognition coupled to the aptamer conformational transition is sensitive enough to characterize the interaction between the L-Tyrosinamide and its aptamer for a wide range of aptamer densities for both platforms. The kinetic data obtained with a 2D-like platform are concordant with previous SPR results obtained on a similar sensor. The kinetic association constant was found to decrease with higher aptamer density leading to a decrease of the L-Tym/aptamer affinity. In addition, we were able to obtain the same K_D than in homogenous medium using SSA sensors with a low aptamer density. This work highlights the crucial influence of aptasensor design on the recognition parameters measured by BLI.

ASSOCIATED CONTENT

Supporting Information

The Supporting Information is available free of charge on the ACS Publications website.
Materials and Methods; Figure S1: Sensorgram of L-Tym with a random DNA sequence on SA and SSA sensors; Figure S2: Sensorgram of D-Tym with Apt49 sequence on SA and SSA sensors; Figure S3: Residual plot; Figure S4: Signal to noise ratio; Figure S5: Standard curves for assessment of L-Tym concentration using SSA sensors; Figure S6: Comparison of SPR and BLI kinetic rate constants on 2D sensors; Table S1: LOD and LOQ of the sensors.

AUTHOR INFORMATION

Corresponding Author

Nicolas Spinelli, + 33 4 56 52 08 33, nicolas.spinelli@univ-grenoble-alpes.fr;
Angéline Van der Heyden, + 33 4 56 52 08 14, angeline.van-der-heyden@univ-grenoble-alpes.fr
Jérôme Dejeu, + 33 4 56 52 08 13, jerome.dejeu@univ-grenoble-alpes.fr

Author Contributions

‡These authors contributed equally.

ACKNOWLEDGMENT

This work was partially supported by the French National Agency (ANR) under ECSTASE, Contract ANR-10-blan-1517, (Rational design of a sensitive and enantiospecific electrocatalytically-amplified aptasensor for amphetamine derivatives drugs), under ARCANE and CBH-EUR-GS (ANR-17-EURE-0003) and the University Grenoble Alpes. The authors wish to acknowledge the support from the ICMG (FR2607) Chemistry Nanobio Platform, Grenoble. Prof. P. Labbé is acknowledged for fruitful discussions.

REFERENCES

(1) Concepcion, J.; Witte, K.; Wartchow, C.; Choo, S.; Yao, D.; Persson, H.; Wei, J.; Li, P.; Heidecker, B.; Ma, W. et al. Label-Free Detection of Biomolecular Interactions Using BioLayer Interferometry for Kinetic Characterization. Comb. Chem. High Throughput Screening 2009, 12, 791-800.

(2) Apiyo, D. O. Chapter 10 Biolayer Interferometry (Octet) for Label-Free Biomolecular Interaction Sensing. In Handbook of Surface Plasmon Resonance (2), The Royal Society of Chemistry: 2017; pp 356-397.

(3) Laigre, E.; Goyard, D.; Tiertant, C.; Dejeu, J.; Renaudet, O. The Study of Multivalent Carbohydrate–Protein Interactions by Bio-Layer Interferometry. Org. Biomol. Chem. 2018, 16, 8899-8903.

(4) Peltomaa, R.; Glahn-Martínez, B.; Benito-Peña, E.; Moreno-Bondi, M. C. Optical Biosensors for Label-Free Detection of Small Molecules. Sensors 2018, 18, 4126.

(5) Zhang, Y.; Wang, Y.; Bao, C.; Xu, Y.; Shen, H.; Chen, J.; Yan, J.; Chen, Y. Metformin Interacts With AMPK Through Binding to γ Subunit. Mol. Cell. Biochem. 2012, 368, 69-76.

(6) Zhu, Z.; Feng, M.; Zuo, L.; Zhu, Z.; Wang, F.; Chen, L.; Li, J.; Shan, G.; Luo, S.-Z. An Aptamer Based Surface Plasmon Resonance Biosensor for the Detection of Ochratoxin A in Wine and Peanut Oil. Biosens. Bioelectron. 2015, 65, 320-326.

(7) Yang, X. Y.; He, K.; Pan, C. S.; Li, Q.; Liu, Y. Y.; Yan, L.; Wei, X. H.; Hu, B. H.; Chang, X.; Mao, X. W. et al. 3, 4-dihydroxyl-phenyl Lactic Acid Restores NADH Dehydrogenase 1 Alpha Subunit 10 to Ameliorate Cardiac Reperfusion Injury. Sci Rep 2015, 5, 10739.

(8) Dai, F.; Chen, Y.; Huang, L.; Wang, J.; Zhang, T.; Li, J.; Tong, W.; Liu, M.; Yi, Z. A Novel Synthetic Small Molecule YH-306 Suppresses Colorectal Tumour Growth and Metastasis via FAK Pathway. J. Cell. Mol. Med. 2015, 19, 383-395.

(9) Grimley, E.; Liao, C.; Ranghini, E. J.; Nikolovska-Coleska, Z.; Dressler, G. R. Inhibition of Pax2 Transcription Activation with a Small Molecule that Targets the DNA Binding Domain. ACS Chem. Biol. 2017, 12, 724-734.

(10) Du, Y.; Dong, S. Nucleic Acid Biosensors: Recent Advances and Perspectives. Anal. Chem. 2017, 89, 189-215.

(11) Zhou, W.; Jimmy Huang, P.-J.; Ding, J.; Liu, J. Aptamer-Based Biosensors for Biomedical Diagnostics. Analyst 2014, 139, 2627-2640.

(12) Pfeiffer, F.; Mayer, G. Selection and Biosensor Application of Aptamers for Small Molecules. Front. Chem. 2016, 4.

(13) Haddache, F.; Le Goff, A.; Spinelli, N.; Gairola, P.; Gorgy, K.; Gondran, C.; Defrancq, E.; Cosnier, S. A Label-Free Photoelectrochemical Cocaine Aptasensor Based on an Electropolymerized Ruthenium-Intercalator Complex. Electrochim. Acta 2016, 219, 82-87.

(14) Kazane, I.; Gorgy, K.; Gondran, C.; Spinelli, N.; Zazoua, A.; Defrancq, E.; Cosnier, S. Highly Sensitive Bisphenol-A Electrochemical Aptasensor Based on Poly(Pyrrole-Nitrilotriacetic Acid)-Aptamer Film. Anal. Chem. 2016.

(15) Kim, S. H.; Thoa, T. T. T.; Gu, M. B. Aptasensors for Environmental Monitoring of Contaminants in Water and Soil. Curr. Opin. Environ. Sci. Health 2019, 10, 9-21.

(16) Oueslati, R.; Cheng, C.; Wu, J.; Chen, J. Highly Sensitive and Specific On-Site Detection of Serum Cocaine by a Low Cost Aptasensor. Biosens. Bioelectron. 2018, 108, 103-108.

(17) Ye, W.; Liu, T.; Zhang, W.; Zhu, M.; Liu, Z.; Kong, Y.; Liu, S. Marine Toxins Detection by Biosensors Based on Aptamers. Toxins 2019, 12, 1.

(18) Gao, S.; Hu, B.; Zheng, X.; Cao, Y.; Liu, D.; Sun, M.; Jiao, B.; Wang, L. Gonyautoxin 1/4 Aptamers with High-Affinity and High-Specificity: From Efficient Selection to Aptasensor Application. Biosens. Bioelectron. 2016, 79, 938-944.

(19) Ouyang, S.; Hu, B.; Zhou, R.; Liu, D.; Peng, D.; Li, Z.; Li, Z.; Jiao, B.; Wang, L. Rapid and Sensitive Detection of Nodularin-R in Water by a Label-Free BLI Aptasensor. Analyst 2018, 143, 4316-4322.

(20) Li, Z.; Hu, B.; Zhou, R.; Zhang, X.; Wang, R.; Gao, Y.; Sun, M.; Jiao, B.; Wang, L. Selection and Application of Aptamers with High-Affinity and High-specificity Against Dinophysistoxin-1. RSC Adv. 2020, 10, 8181-8189.

(21) Osypova, A.; Thakar, D.; Dejeu, J.; Bonnet, H.; Van der Heyden, A.; Dubacheva, G. V.; Richter, R. P.; Defrancq, E.; Spinelli, N.; Coche-Guérente, L. et al. Sensor Based on Aptamer Folding to Detect Low-Molecular Weight Analytes. Anal. Chem. 2015, 87, 7566-74.

(22) Dejeu, J.; Bonnet, H.; Spinelli, N.; Defrancq, E.; Coche-Guérente, L.; Van der Heyden, A.; Labbé, P. Impact of Conformational Transitions on SPR Signals—Theoretical Treatment and Application in Small Analytes/Aptamer Recognition. J. Phys. Chem. C 2018, 122, 21521-21530.

(23) MacDonald, H.; Bonnet, H.; Van der Heyden, A.; Defrancq, E.; Spinelli, N.; Coche-Guérente, L.; Dejeu, J. Influence of Aptamer Surface Coverage on Small Target Recognition: A SPR and QCM-D Comparative Study. J. Phys. Chem. C 2019, 123, 13561-13568.

(24) Ruta, J.; Perrier, S.; Ravelet, C.; Fize, J.; Peyrin, E. Noncompetitive Fluorescence Polarization Aptamer-based Assay for Small Molecule Detection. Anal. Chem. 2009, 81, 7468-7473.

(25) Weynand, J.; Bonnet, H.; Loiseau, F.; Ravanat, J.-L.; Dejeu, J.; Defrancq, E.; Elias, B. Targeting G-Rich DNA Structures with Photoreactive Bis-Cyclometallated Iridium(III) Complexes. Chem. Eur. J. 2019, 25, 12730-12739.

(26) Kamat, V.; Rafique, A. Designing Binding Kinetic Assay on the Bio-Layer Interferometry (BLI) Biosensor to Characterize Antibody-Antigen Interactions. Anal. Biochem. 2017, 536, 16-31.

(27) Lin, P.-H.; Yen, S.-L.; Lin, M.-S.; Chang, Y.; Louis, S. R.; Higuchi, A.; Chen, W.-Y. Microcalorimetrics Studies of the Thermodynamics and Binding Mechanism Between L-Tyrosinamide and Aptamer. J. Phys. Chem. B 2008, 112, 6665-6673.

(28) Challier, L.; Mavre, F.; Moreau, J.; Fave, C.; Schoellhorn, B.; Marchal, D.; Peyrin, E.; Noel, V.; Limoges, B. Simple and Highly Enantioselective Electrochemical Aptamer-Based Binding Assay for Trace Detection of Chiral Compounds. Anal. Chem. 2012, 84, 5415-5420.

SYNOPSIS TOC (Word Style “SN_Synopsis_TOC”).